DALTON

Dynamic disorder in crystalline $[Fe_2Os(CO)_{12}]$ and direct evidence for rotation of the Fe_2Os triangle in the solid state from variable temperature X-ray diffraction and ^{13}C MAS NMR studies †

Louis J. Farrugia,*[a] Andrew M. Senior,[a] Dario Braga,[b] Fabrizia Grepioni,*[b] A. Guy Orpen[c] and John G. Crossley[c]

[a] *Department of Chemistry, University of Glasgow, Glasgow G12 8QQ, UK*
[b] *Dipartimento di Chimica 'G. Ciamician', Università di Bologna, Via Selmi 2, 40126 Bologna, Italy*
[c] *Department of Chemistry, University of Bristol, Cantocks Close, Bristol BS8 1TS, UK*

Single-crystal X-ray diffraction data have been collected for $[Fe_2Os(CO)_{12}]$ at 120, 223, 288, 292 and 323 K. The two studies at ambient temperature (288 and 292 K) reveal a $\approx 12:1$ disorder of the metal triangle as previously reported. At the two lowest temperatures there is no evidence of disorder, while at 323 K the ratio of the major : minor component of disorder decreases significantly to $\approx 1.4:1$. Data collected on the same crystal specimens indicate unequivocally that this disorder is dynamic in nature. Two-dimensional exchange and one-dimensional variable-temperature ^{13}C magic angle spinning (MAS) NMR spectroscopy showed that carbonyl exchange is rapid above 306 K in the crystalline solid. Two independent exchange processes of similar energy are observed. The first is consistent with the crystallographic evidence, and involves an 'in-plane' rotation of the Fe_2Os triangle in steps of 60° within a relatively rigid icosahedral carbonyl manifold. The second involves localised axial–equatorial exchange in the $Os(CO)_4$ group. The Os L_{III} and Fe K edge X-ray absorption fine structure spectra are consistent with identical structures being present in tetrahydrofuran solution and in the solid phase.

One of the more fascinating properties of transition-metal cluster compounds is their conformational non-rigidity, which very often manifests itself in solution,[1] but has also been observed in the solid state.[2] Apart from the intrinsic interest in fluxional behaviour, studies on the dynamics of molecular clusters, particularly in the solid state, may also shed light on the important problem of adsorbate mobility on metal surfaces.[3] There is now a substantial body of work delineating dynamic processes in the solid state in organometallic crystals in general,[4] and in some cluster compounds.[2]

One classic example of a fluxional cluster is $[Fe_3(CO)_{12}]$ **1** which, in solution, exhibits a single ^{13}C NMR resonance[5] for the carbonyl ligands down to −150 °C, indicating an exchange process with a barrier of less than 20 kJ mol^{-1}. Since this barrier is so small, 'static' ^{13}C NMR spectra of **1** in solution have never been obtained, and definitive conclusions regarding the fluxional mechanism in this phase cannot be made. The solid-state ^{13}C MAS (magic angle spinning) NMR spectrum of **1**[6] is also temperature dependent,[6a] but the interpretation of these observations is still controversial. Three different models have been proposed to rationalise the solid-state dynamic behaviour: (*a*) an in-plane 60° rotational jump of the Fe_3 triangle within an essentially rigid carbonyl manifold which results in pairwise exchange of CO ligands;[6a,c] (*b*) a librational motion of the metal triangle[7] about the molecular pseudo-two-fold axis, again within an essentially rigid carbonyl manifold (this motion converts the C_{2v} bridged structure to a D_3 all-terminal structure, an idea originally proposed in 1976 by Johnson[7a] to explain the solution fluxionality of **1** and (*c*) concerted shifts of the bridging carbonyl ligands along metal edges without intermetallic migration of CO.[8]

We have recently reported[9] a variable-temperature X-ray diffraction study on cluster **1** which was carried out in order to shed more light on the question of the solid-state dynamic behaviour of this molecule. We did not observe any phase transition down to 100 K, so that the well known[10] 1:1 disordered 'star of David' pattern for the metal atoms is retained, due to the presence of the inversion centre in the space group $P2_1/n$. Both of the bridging carbonyl groups become more symmetrical at low temperatures, so that at 100 K the molecule attains almost exact C_{2v} symmetry. These studies suggest a small energy difference between the symmetric and asymmetric carbonyl bridge-bonding modes.

We have now carried out a variable-temperature X-ray diffraction study on the closely related molecule $[Fe_2Os(CO)_{12}]$ **2**. The structure of this cluster has been previously determined by Churchill and Fettinger.[11] Both the *molecular* and *crystal* structures are similar to those found for **1**, and the relationships between the two structures have been discussed in some detail by these authors.[11] The most important difference lies in the fact that, for **2**, the 'star of David' disorder of the metal atoms is not constrained to be 1:1, since there is no inversion centre at the centroid of the Fe_2Os triangle. The molecule crystallises in the non-centrosymmetric space group Pn, and in their room-temperature study Churchill and Fettinger[11] reported a $\approx 12:1$ disorder in the metal atom positions.

In this paper we demonstrate unequivocally that this disorder arises from a dynamic process in the solid state. Taken together with the variable-temperature ^{13}C MAS NMR data on cluster **2**, our results provide direct evidence for an 'in-plane' rotation of the Fe_2Os triangle within a relatively rigid carbonyl ligand manifold. We also report Os L_{III} and Fe K edge EXAFS (extended X-ray absorption fine structure) spectra, which indicate that identical structures are present in the solution and solid phases. Part of this work has been previously communicated.[12]

Results and Discussion

Crystallographic studies

Single-crystal X-ray diffraction data were collected for $[Fe_2Os(CO)_{12}]$ at 120, 223 and 323 K, and also at ambient temperature (288 K at Bologna, and 292 K at Glasgow) to

† Basis of the presentation given at Dalton Discussion No. 1, 3rd–5th January 1996, University of Southampton, UK.

provide a baseline comparison with the structural determination at 297 K of Churchill and Fettinger.[11] In summary our results show that at 120 and 223 K there is no trace of any disorder, and at 323 K the ratio of the major:minor components of disorder decreases significantly to $\approx 1.4:1$. The same *molecular* structure is retained at all temperatures.

In order to demonstrate the reversibility of the dynamic disorder, data were also collected at room temperature on the same crystal specimen used for the 120 K study. Data recollection at 292 K was commenced immediately after a 12 h period to allow for slow thermal annealing. The results obtained from this data set were identical to those given here for the 292 K data set obtained from a different crystal specimen, and are not reported in any detail. The disappearance and reappearance of the disorder in the same crystal specimen provides categorical proof of the dynamic nature of the disorder.

Structural analyses at room temperature

The results of our analyses of diffraction data collected at 292 and 288 K are essentially identical to those reported by Churchill and Fettinger[11] and only salient points will be discussed. Some important bond distances are presented in Table 1, together with those obtained from the Churchill and Fettinger study.[11]

The structure contains two crystallographically independent molecules of $[Fe_2Os(CO)_{12}]$ in the asymmetric unit, both of which show a disorder in the metal positions (Figs. 1 and 2). For both of the independent molecules, one of the positions within the minor component metal triangle has considerably greater electron density than the other two, and this position was initially assigned to an osmium atom. The major:minor populations were refined independently in the two molecules, and for the structure determination at 292 K this gave populations of 10.1:1 for molecule 1 and 13.3:1 for molecule 2. The mean is the same as that reported by Churchill and Fettinger.[11] Due to the low population of the minor metal triangle components, no attempt was made to determine their corresponding light atom positions.

The disordered structures illustrated in Figs. 1 and 2 indicate that there must be a 180° rotational jump of the Fe_2Os triangle to interconvert the major and minor orientations. In order to ascertain whether such a rotational jump occurred stepwise *via* 60° rotational jumps, a careful refinement was carried out on the data set collected at 292 K to examine for possible Fe/Os disorder at each of the metal sites. One of the proposed mechanisms for solid-state fluxionality of $[Fe_3(CO)_{12}]$ involves a 60° in-plane rotational jump of the Fe_3 triangle,[6a,c] though of course it is not possible, in this case, to distinguish between ± 60 or 180° jumps from crystallographic evidence alone, since these rotations are degenerate. However the replacement of one iron atom by an osmium atom removes this degeneracy. For the major components of both molecules 1 and 2, and for the minor component of 2, there was no evidence for any such Fe/Os disorder. However, for the minor component in molecule 1 the refinement indicated that the site labelled Os(1A) consists of $\frac{2}{3}$Os and $\frac{1}{3}$Fe, while the two sites Fe(1B) and Fe(1C) are $\frac{2}{3}$Fe and $\frac{1}{3}$Os. In view of the low overall population of the minor components at this temperature, this observation must be treated with some caution.

The other important point of interest concerns the relative orientations of the two triangles in each of the independent molecules. In cluster **1** the two 'star of David' positions are constrained to be coplanar in view of the generating centre of inversion.[10] This is not the case with **2**. As can be seen from Figs. 1 and 2, the minor component triangle is not coplanar with the major component triangle for both of the independent molecules. The deviations of the minor component triangle from the mean plane defined by the major component for the analyses at 288, 292 and 323 K are given in Table 2, with the results of the analysis by Churchill and Fettinger[11] for comparison. For all the structural analyses around room temperature, the minor component Os atoms lie close to the major component triangular plane, while the two minor component Fe atoms lie above and below this plane for both independent molecules. This suggests that the atomic motion necessary to interconvert the major and minor orientations of $[Fe_2Os(CO)_{12}]$ involves not only an in-plane triangular rotation, but also a tilting motion of the triangles, primarily affecting the two iron atoms.

Low-temperature structural analyses

The two low-temperature structural analyses carried out at 223 and 120 K present essentially the same picture as each other. There is no trace of a secondary metal triangle position, as we have previously clearly shown[12] from Fourier sections through the Os(11)–Fe(11)–Fe(12) triangle at 292 and 120 K. We have observed no phase change down to 100 K, so that at low temperatures the crystal structure consists of an *ordered* arrangement of two independent molecules of cluster **2** in the asymmetric unit.

The metrical parameters for the two independent molecules are very similar at both temperatures, and provide perhaps the best determination of the '$Fe_3(CO)_{12}$' structural archetype. The presence of two molecules in the asymmetric unit also allows an assessment of the importance of packing forces in determining

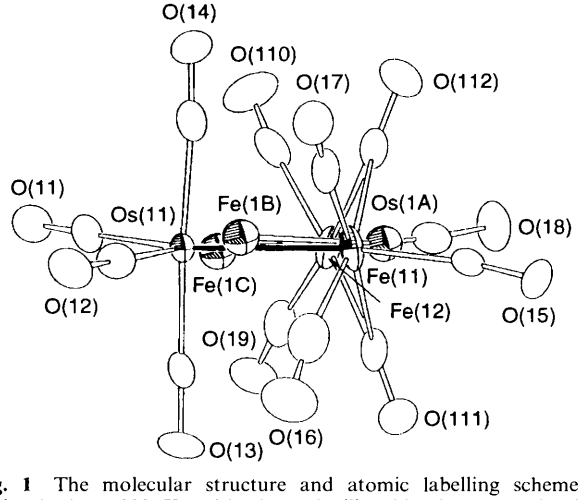

Fig. 1 The molecular structure and atomic labelling scheme of molecule 1 at 292 K, with thermal ellipsoids shown at the 30% probability level

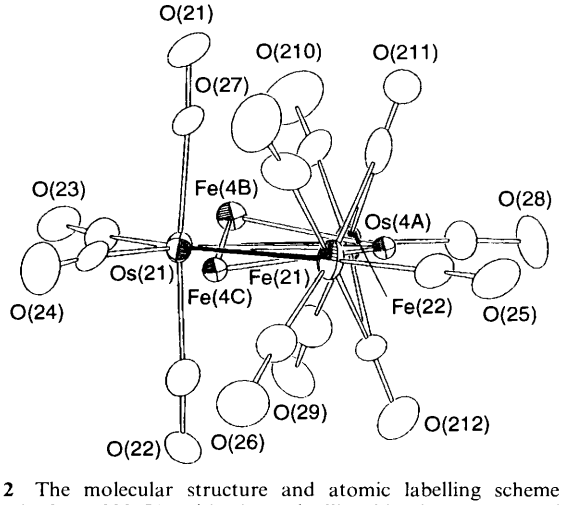

Fig. 2 The molecular structure and atomic labelling scheme of molecule 2 at 292 K, with thermal ellipsoids shown at the 30% probability level

Table 1 Comparison of important bond lengths (Å)

T/K	120	223	288	292	297*	323
Molecule 1						
Os(11)–Fe(11)	2.759(2)	2.759(2)	2.750(3)	2.713(2)	2.735(2)	2.729(10)
Os(11)–Fe(12)	2.770(2)	2.767(2)	2.761(3)	2.741(2)	2.740(3)	2.787(9)
Fe(11)–Fe(12)	2.567(3)	2.571(3)	2.581(3)	2.581(3)	2.589(4)	2.599(11)
Os(1A)–Fe(1B)	—	—	2.67(3)	2.70(2)	2.74(2)	2.65(2)
Os(1A)–Fe(1C)	—	—	2.68(3)	2.70(2)	2.68(2)	2.71(2)
Fe(1B)–Fe(1C)	—	—	2.62(4)	2.64(2)	2.58(3)	2.50(2)
Fe(11)–C(111)	2.10(1)	2.14(2)	2.26(2)	2.24(2)	2.25(2)	2.24(2)
Fe(11)–C(112)	1.95(1)	1.93(1)	1.92(2)	1.96(2)	1.92(2)	1.98(2)
Fe(12)–C(111)	1.93(1)	1.94(2)	1.97(2)	1.99(2)	1.94(2)	2.06(2)
Fe(12)–C(112)	2.08(1)	2.14(1)	2.24(2)	2.15(2)	2.22(2)	2.17(2)
Molecule 2						
Os(21)–Fe(21)	2.725(2)	2.742(2)	2.715(3)	2.755(2)	2.745(3)	2.717(9)
Os(21)–Fe(22)	2.713(2)	2.716(2)	2.707(3)	2.733(2)	2.746(3)	2.687(10)
Fe(21)–Fe(22)	2.574(3)	2.571(3)	2.581(3)	2.581(3)	2.594(4)	2.549(12)
Os(4A)–Fe(4B)	—	—	2.78(2)	2.80(3)	2.75(3)	2.75(2)
Os(4A)–Fe(4C)	—	—	2.82(3)	2.77(2)	2.82(3)	2.72(2)
Fe(4B)–Fe(4C)	—	—	2.67(3)	2.71(4)	2.58(3)	2.65(2)
Fe(21)–C(211)	2.02(1)	2.06(2)	2.14(2)	2.14(2)	2.08(2)	1.91(4)
Fe(21)–C(212)	1.96(1)	1.97(2)	1.90(2)	1.98(2)	1.94(2)	1.91(4)
Fe(22)–C(211)	2.00(1)	2.00(2)	2.01(2)	2.08(2)	2.05(2)	1.82(3)
Fe(22)–C(212)	2.05(1)	2.06(1)	2.08(2)	2.08(2)	2.12(2)	1.90(3)

* Data from Churchill and Fettinger.[11]

Table 2 Deviations from the selected mean planes

		Deviation/Å			
Plane	Atom	288	292	297*	323 K
Os(11), Fe(11), Fe(12)	Os(1A)	−0.07	−0.07	−0.07	−0.05
	Fe(1B)	−0.19	−0.19	−0.21	−0.20
	Fe(1C)	0.31	0.07	0.13	−0.08
Os(21), Fe(21), Fe(22)	Os(4A)	−0.06	−0.07	−0.08	−0.13
	Fe(4B)	−0.02	−0.36	−0.23	−0.08
	Fe(4C)	0.01	0.16	0.10	−0.09

* Data taken from Churchill and Fettinger.[11]

the fine structural details. Cluster **2** has essentially C_2 symmetry, but the two independent molecules differ in the degree of asymmetry of the carbonyl bridges, and in the torsional conformation of the $Os(CO)_4$ group (see Fig. 3). In molecule 1 the carbonyl bridges are more asymmetric, and the $Os(CO)_4$ unit is twisted out of the Fe_2Os plane to a greater degree than in molecule 2, and this difference is retained throughout the temperature range we have investigated. This may be taken to indicate that both of these distortions represent soft modes. One of us has previously noted a similar variation in the torsional conformation of the $Os(CO)_4$ group in the butterfly clusters $[Os_3Pt(\mu\text{-}H)_2(CO)_{10}(PR_3)_2]$,[13] and this distortion is precisely the motion necessary to convert the D_{3h} structure of $[Os_3(CO)_{12}]$ to the D_3 form observed in several phosphine derivatives of $[M_3(CO)_{12}]$ (M = Ru or Os).[7d,14,15] The relevance of the D_3 structure of $[M_3(CO)_{12}]$ to the solution fluxionality of these molecules has been discussed by Johnson and co-workers.[7c,d]

High-temperature structural analysis

The analysis of the data set collected at 323 K was less straightforward than the others. In part this was due to the greater disorder, but also to the poorer quality data. This is to be expected, due to the decrease in the Bragg intensities and the increase in thermal diffuse scattering with temperature. The most striking effect of increasing the temperature is the very significant decrease in the ratio of the major : minor component. These population ratios refined to 1.35 : 1 for molecule 1 and 1.47 : 1 for molecule 2, giving a mean ratio of ≈1.4 : 1.

During the initial stages of refinement an investigation was undertaken into possible Fe/Os disorder in the metal sites, similar to that performed for the data set collected at 292 K. With the higher abundance of the secondary component any conclusions should be more reliable. This investigation revealed that the sites labelled as Fe contained *at most* a few percent of an Os atom, and therefore it was decided to assign only one chemical element to each of the metal positions for the purposes of refinement. Nevertheless the crystallographic evidence at 323 K is consistent with a small population of osmium in the iron sites, and *vice versa*. This point is important for an understanding of the variable-temperature ^{13}C NMR data (see below).

Since both images of the metal triangle have sufficiently high populations, it is possible to refine them successfully with anisotropic thermal parameters. The thermal ellipsoids for the metal atoms in both independent molecules are shown in Fig. 4. As previously noted by Churchill and Fettinger[11] for **2**, and similarly to the situation which has been discussed for **1**,[7c,d,9] the major vibrational amplitude of the iron atoms appears to be normal to the metal triangular plane, while the thermal parameters of the osmium atoms are reasonably isotropic. It is possible that the anisotropic thermal parameters derived from the least-squares refinement may represent actual thermal motion of the metal atoms. In this case, it suggests that there is a low-energy librational motion about the C_2 axes of the metal triangles.[7c,d,9] Alternatively, the thermal parameters may represent a convolution of a further disorder, wherein the iron atoms actually have two positions, below and above the averaged plane. These two positions would be too close to be resolved in the present study, and we cannot distinguish between these two possibilities. However, this disorder model is consistent with the disposition of the minor component triangles in the structure at room temperature (see above), and would also explain some of the rather short Os–Fe and Fe–Fe distances (see Table 1) which are found at 323 K.

Finally it is of some interest that a unit cell for cluster **2** was determined at 373 K, prior to an attempted data collection. A phase transition occurs, and the new crystal system is monoclinic with unit-cell parameters $a = 8.47(1)$, $b = 11.46(2)$,

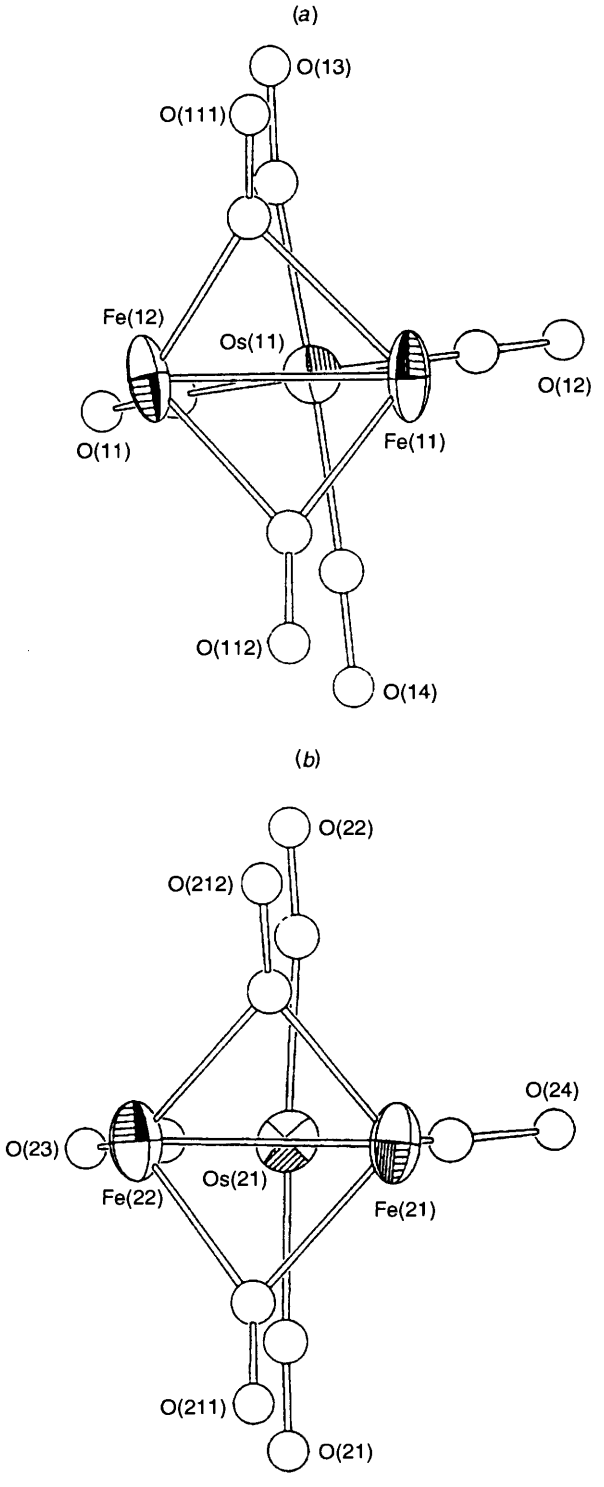

Fig. 3 The orientation of the $Os(CO)_4$ groups and the bridging carbonyls viewed along the Fe_2Os triangle (major component, 292 K), (*a*) for molecule 1 and (*b*) for molecule 2

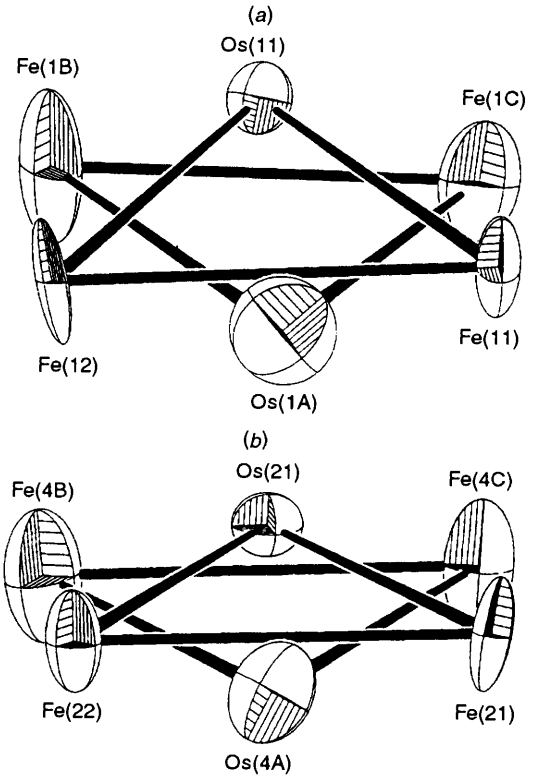

Fig. 4 Thermal ellipsoids for the disordered metal triangles at 323 K shown at the 30% probability level, (*a*) for molecule 1 and (*b*) for molecule 2

c = 8.949(8) Å, β = 96.59(9)°. The b axis is thus halved, and this unit cell is very similar to that of $[Fe_3(CO)_{12}]$[9,10] which suggests that a full reorientational motion of the metal triangle may be occurring, giving an averaged structure similar to that of $[Fe_3(CO)_{12}]$. Unfortunately, crystal decomposition was rapid at this temperature, and it was not possible to determine the space group.

General comments on the structural determinations

In contrast to the previous variable-temperature study[9] on $[Fe_3(CO)_{12}]$, there does not appear to be any unequivocal pattern of structural changes with temperature for $[Fe_2Os(CO)_{12}]$. The bond lengths given in Table 1 show few consistent trends. For both independent molecules the Fe–Fe distance increases with increasing temperature. However, while the Os–Fe distances in molecule 1 show an overall decrease with increasing temperature, the opposite trend is observed in molecule 2. The *mean* Fe–Os distances measured for the major image in the data sets between 120 and 297 K are 2.750 Å for molecule 1 and 2.730 Å for molecule 2. However, there are significant variations in these chemically equivalent Os–Fe distances, about ten times the estimated standard deviation (e.s.d.), which are difficult to rationalise. Although a similar effect in other systems has been noted[16] which demonstrates that metal–metal bonds are very soft, there are other possible causes. These include metal site disorder, which we cannot evaluate accurately, as well as other systematic experimental errors.

As in previous cases where the packing of cluster structures containing two independent molecules in the asymmetric unit has been examined,[16b,17] it is found that the molecules pack in alternate double layers which contain only one of the independent molecules. In the present structure these layers lie perpendicular to the crystallographic b axis, see Fig. 5. This may be regarded in a sense as a 'cocrystal' of the two independent molecules.

Structure of $[Fe_2Os(CO)_{12}]$ in solution

The reported solution IR spectrum of cluster **2** in hexane[18] shows eight ν(CO) bands in the region 2119–1840 cm^{-1}. The two bands at 1865 and 1840 cm^{-1} are both weak and broad, and may be ascribed to the bridging carbonyls. This spectrum is reasonably consistent with the determined solid-state structure. Compound **2** in CD_2Cl_2 solution shows a single sharp resonance at δ 200.1 in the ^{13}C NMR spectrum at room temperature. This signal is very close to the weighted mean (δ 201.6, see below) of the solid-state ^{13}C resonances and indicates

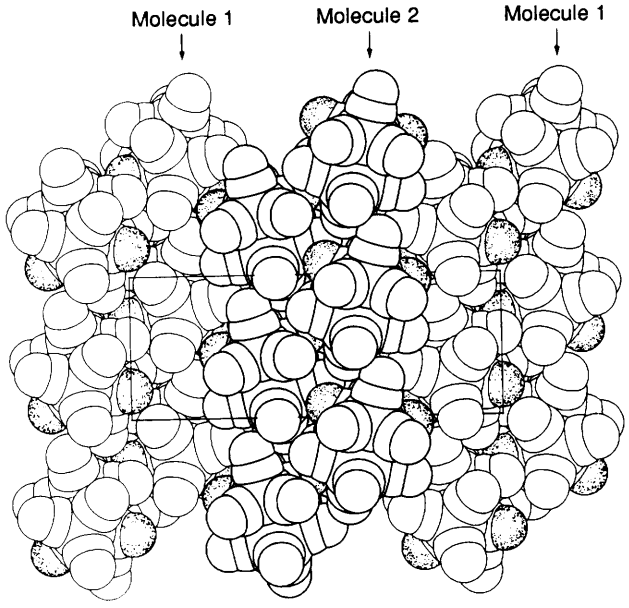

Fig. 5 Space-filling view of the unit cell of $[Fe_2Os(CO)_{12}]$, showing the layers of pairs of the independent molecules packed together. The oxygen atoms of the bridging carbonyls are shaded

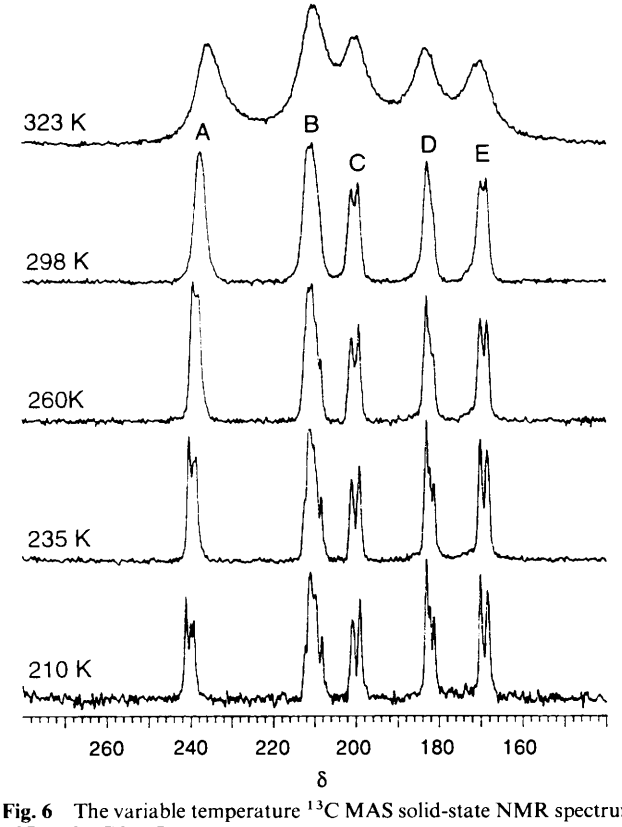

Fig. 6 The variable temperature ^{13}C MAS solid-state NMR spectrum of $[Fe_2Os(CO)_{12}]$

complete carbonyl scrambling. On cooling this singlet broadens, and is lost into the baseline at around 193 K. While no information concerning the mechanism of carbonyl scrambling can be obtained from these data, it is clear that the activation energy of the dynamic process(es) must be greater than for **1**, since this latter molecule exhibits a sharp singlet in the ^{13}C NMR spectrum[5] down to 120 K.

In order to obtain further information regarding the solution structure of cluster **2**, Os L_{III} edge and Fe K edge EXAFS spectra in the solid phase and in tetrahydrofuran (thf) solution were obtained. These studies are described in detail in the Experimental section, and the resultant molecular dimensions are given in Table 3. In summary, there are no significant differences between the EXAFS models in the solution or solid phase, for either the Fe K edge or the Os L_{III} edge data. There are no trends in the parameters of the models at different temperatures, but there is good agreement between the EXAFS and single-crystal diffraction data, and insofar as the EXAFS data determine the metal–ligand environment, the results are consistent with the same structure being maintained in both solid and thf solution.

Solid-state ^{13}C MAS NMR studies

The crystallographic results presented above clearly indicate a reversible process which involves a 180° rotation of the Fe_2Os triangle relative to the crystal lattice. It is not clear, however, whether the whole molecule of $[Fe_2Os(CO)_{12}]$ rotates intact within the lattice, or whether it is just the metal triangle which rotates within a relatively rigid carbonyl manifold. Since X-ray crystallography cannot distinguish atoms of the same elemental type from each other, this method can provide no answer to this question. We have therefore examined the solid-state NMR behaviour of cluster **2**, since the NMR technique is sensitive to the fate of individual atomic nuclei if their chemical shift changes.

The variable-temperature ^{13}C MAS NMR spectrum of a ^{13}CO-enriched sample of $[Fe_2Os(CO)_{12}]$ is shown in Fig. 6, and the parameters are given in Table 4. At room temperature there are five groups of broad signals A–E at *ca.* δ 237, 210.5, 199.7, 182.5 and 169.2 in the relative intensity ratio 1 : 2 : 1 : 1 : 1. On cooling, further fine structure becomes apparent. The relative intensities given in Table 4 for the signals at 210 K were obtained by Lorenzian deconvolution of the total bandshape. In particular, the set of signals A at *ca.* δ 240 is resolved into three singlets at δ 241.0, 239.9 and 239.1 (2 : 1 : 1 intensity ratio). These may be attributed to the four *crystallographically* distinct bridging carbonyls within the two independent molecules, with one accidental degeneracy. Likewise, the set of signals D are resolved into three singlets (2 : 1 : 1), while the other signals show a less satisfactory resolution.

The solid-state spectra also provide useful information regarding the chemical shift anisotropies (CSAs) of the carbonyl sites. The shielding tensors given in Table 4 were calculated by the method of Maricq and Waugh[20] from the spectrum at 298 K, with sufficient line broadening being applied to remove the fine splittings. The values obtained are hence *averages* for all the carbonyls in each of the five chemically distinct sites. This is a satisfactory approximation, since Walter *et al.*[6c] have shown that carbonyl sites which are chemically equivalent, but merely crystallographically inequivalent, have essentially identical CSAs. The CSA of signal A is substantially smaller than those for the other resonances, and this provides further confirmation that this signal is due to the bridging carbonyls. It is now well established that bridging carbonyl ligands have much smaller CSAs than terminal carbonyls.[6c,21] In addition, Hawkes *et al.*[21b] have noted that the σ_{33} magnitudes are much smaller for symmetric bridging carbonyls than for terminal carbonyls, and this is also observed in our case for signal A.

The set of signals B around δ 210.5 are assigned to the eight radial carbonyl ligands on the two Fe atoms, and the signals C centred at δ 199.7 to the four equatorial carbonyls on the Fe atoms. The two signals D and E centred at δ 182.5 and 169.2 are ascribed to the axial and equatorial carbonyls respectively on the $Os(CO)_4$ groups. These latter chemical shifts are virtually identical to those reported by Walter *et al.*[6c] (δ 182.3 and 170.4) and Aime *et al.*[22] (δ ≈ 182 and ≈169) for $[Os_3(CO)_{12}]$. All groups of signals are unambiguously assigned, and the spectrum at 210 K is therefore entirely consistent with a static molecular and crystal structure, as is indicated by the X-ray analysis at 233 K.

Table 3 Details of EXAFS data analysis for $[Fe_2Os(CO)_{12}]$ **2**

		Fe K edge EXAFS													
XRD[a]			Contact	Solid, 300 K		Solid, 243 K		Solid, 223 K		Solid, 203 K		Solid, 110 K		Solution, 300 K	
Contact	R/Å	Shell	N (atom)	R/Å	σ/Å²	R/Å	σ/Å²	R/Å	σ/Å²	R/Å	σ/Å²	R/Å	σ/Å²	R/Å	σ/Å²
Fe–C	1.803	1	3 C	1.804(4)[b]	0.0060(7)	1.811(5)	0.0055(9)	1.807(5)	0.0050(8)	1.811(4)	0.0041(7)	1.811(6)	0.006(1)	1.814(4)	0.0036(7)
Fe–Fe	2.591	2	1 Fe	2.53(1)	0.015(2)	2.55(1)	0.013(2)	2.56(1)	0.010(2)	2.56(1)	0.010(2)	2.546(7)	0.005(1)	2.57(3)	0.0026(10)
Fe–Os	2.742	3	1 Os	2.752(4)	0.066(6)	2.756(3)	0.0046(4)	2.752(3)	0.0047(5)	2.765(3)	0.0037(3)	2.748(2)	0.0023(3)	2.762(4)	0.0047(6)
Fe–O	2.934	4	3 O	2.907(6)	0.009(1)	2.924(9)	0.011(2)	2.917(9)	0.012(2)	2.919(4)	0.013(2)	2.92(1)	0.011(2)	2.916(8)	0.010(2)
Correlations between R and σ > 0.50				σ4–σ2 −0.67, σ1–R1 −0.87, σ4–R3, −0.51, σ3–R3 −0.52, σ4–R4 −0.84, R4–R2 −0.59, σ2–R2 −0.93, σ4–R2 0.85		σ4–σ2 −0.79, σ1–R1 −0.83, σ3–R3 −0.58, σ4–R3 −0.64, σ2–R4 0.54, σ4–R4 −0.84, R4–R2 −0.64, R3–R2 −0.58, σ2–R2 −0.97, σ4–R2 0.89		σ3–σ2 −0.57, σ4–σ2 −0.79, σ1–R1 −0.85, σ2–R3 0.53, σ4–R3 −0.65, σ3–R3 −0.68, σ2–R4 0.57, σ4–R4 −0.85, R4–R2 −0.66, R3–R2 −0.61, σ2–R2 −0.96, σ3–R2 0.56, σ4–R2 0.89		σ4–σ2 −0.74, σ1–R1 −0.85, σ4–R3 −0.57, σ3–R3 −0.59, σ2–R4 0.52, σ4–R4 −0.83, R4–R2 −0.52, σ2–R2 −0.95, σ4–R2 0.87, σ2–R4 −0.63		σ4–σ2 −0.54, σ1–R1 −0.74, σ4–R3 −0.56, σ3–R3 −0.51, σ4–R4 −0.80, R3–R2 −0.52, σ2–R2 −0.87, σ4–R2 0.77		σ4–σ2 −0.68, σ1–R1 −0.82, σ4–R4 −0.74, σ2–R2 −0.95, σ4–R2 0.84
k_{max}/Å^{-1}				15.75		16.80		16.68		16.80		16.75		15.60	
R (%)[c]				13.2		18.4		17.9		16.1		16.4		10.8	
R' (%)				7.37		13.0		13.3		10.6		8.44		6.83	

		Os L_{III} edge EXAFS											
XRD[a]			Contact	Solid, 300 K		Solid, 223 K		Solid, 110 K		Solution, 300 K		Solution, 145 K	
Contact	R/Å	Shell	N (atom)	R/Å	σ/Å²	R/Å	σ/Å²	R/Å	σ/Å²	R/Å	σ/Å²	R/Å	σ/Å²
Os–C	1.946	1	4 C	1.943(3)[b]	0.0035(5)	1.944(5)	0.0052(9)	1.943(3)	0.0038(5)	1.935(2)	0.0033(4)	1.939(3)	0.0026(4)
Os–Fe	2.742	2	2 Fe	2.730(4)	0.0067(6)	2.720(6)	0.0084(9)	2.734(2)	0.0029(3)	2.747(4)	0.0111(8)	2.735(3)	0.0067(6)
Os–O	3.063	3	4 O	3.062(4)	0.0051(6)	3.058(4)	0.0040(7)	3.068(4)	0.0050(7)	3.060(4)	0.0075(6)	3.055(3)	0.0047(6)
Os–C	4.3	4	4 C	not fitted		not fitted		not fitted		4.33(2)	0.003(3)	4.32(1)	0.0046(5)
Correlations between R and σ > 0.50				σ1–R1 −0.85, σ3–R2 0.65, σ2–R2 −0.83, σ3–R3 −0.72		σ1–R1 −0.83, σ3–R2 0.65, σ2–R2 −0.90, σ3–R3 −0.60		σ1–R1 −0.84, σ3–R2 0.75, σ2–R2 −0.74, σ3–R3 −0.77		σ1–R1 −0.85, σ2–R2 −0.86, σ3–R3 −0.82, σ4–R4 −0.55		σ1–R1 −0.79, σ2–R2 −0.86, σ3–R3 −0.74	
k_{max}/Å^{-1}				15.90		15.23		16.96		15.93		14.93	
R (%)[c]				15.2		23.3		13.6		8.56		9.33	
R' (%)				7.69		15.6		7.20		5.87		7.69	

[a] The XRD values are distances derived from the crystal structure determination at room temperature, for the major orientation, and are averaged for the two independent molecules and for equivalent distances. [b] The estimated standard deviation in the least significant digit as calculated by EXCURV92[19] model fitting is given in parentheses. We note that such estimates of precision are likely to be underestimates of accuracy and particularly so in cases of high correlation between parameters. [c] Residual indices R and R' were calculated as $R = \Sigma_i[k^3(\chi_i^{obs} - \chi_i^{calc})]^2/\Sigma_i(k^3\chi_i^{obs})^2$, R' as for R, with final model parameters, but with data Fourier filtered with r_{max} 7.5 Å to remove noise.

Table 4 The ^{13}C MAS NMR parameters[a] for $[Fe_2Os(CO)_{12}]$

T/K	δ_{iso}[b]			σ_{11}	σ_{22}	σ_{33}	$\Delta\delta$
298	237(1)			−348.7	−332.2	−30.7	206.5
	210.5(2)			−391.3	−391.3	151	361.6
	199.7(1)			−393.0	−359.4	153.3	353.0
	182.5(1)			−346.0	−346.0	144.5	327.0
	169.2(1)			−330.1	−330.2	152.7	321.9
210	241.0(2)	239.9(1)	239.1(1)				
	212.1	210.9	209.6				
	208.1						
	200.8(2)	199.0(2)					
	182.9(2)	182.2(1)	181.1(1)				
	170.0(2)	168.4(2)					

[a] The convention adopted is that $-\delta_{iso} = \sigma_{iso} = (\sigma_{11} + \sigma_{22} + \sigma_{33})/3$ and $\Delta\delta = \sigma_{33} - \sigma_{iso}$. [b] Relative intensities in parentheses.

On warming from room temperature to 323 K there is a substantial broadening of all signals, indicating the onset of an exchange process involving significant changes in chemical shifts. There are two factors which must be borne in mind in any interpretation of this exchange process, namely the magnitude of the exchange rate constants and the relative 'populations' of the two components. From the crystallographic evidence we can infer that the system is essentially a case of two major 'isomers' of unequal population involved in exchange. If the population of the minor 'isomer' is small compared with that of the major 'isomer' then regardless of the exchange rate constants the line broadening observed for the major 'isomer' will be relatively small. This is the case for solid $[Fe_2Os(CO)_{12}]$ up to 260 K at least. However at 323 K the minor 'isomer' has a significant population, and the exchange between these two 'isomers' results in substantial line broadening.

It seems very likely that the changes observed in the ^{13}C NMR spectrum are correlated with the effects observed in the diffraction experiments, since in both cases the major effects occur in the same temperature range, *i.e.* ≈290 to ≈320 K. All the ^{13}C signals appear to broaden at much the same rate; in particular the group of signals B are also broadened. These results allow us to make some firmer conclusions regarding the dynamic mechanism(s) in the solid state. For instance, a two-fold rotation within the crystal lattice of *intact* molecules of $[Fe_2Os(CO)_{12}]$ about the pseudo-C_3 axis of the metal triangle would not produce any *major* chemical shift changes for the carbonyl ligands, since the lattice effects for chemically identical nuclei in these systems[6c,22] are at most 6–8 ppm. Such a rotation *alone* therefore cannot account for the observed ^{13}C NMR spectra, even though it is consistent with the crystallographic results. Other mechanisms must therefore be operative.

Referring to the labelling scheme in Fig. 1, a *direct* 180° in-plane rotation of the Fe_2Os triangle with a relatively rigid* icosahedral carbonyl polyhedron[23] would result in the carbonyl exchanges C(11)/C(12)↔C(15)/C(18) (*i.e.* E↔C) and C(111)/C(112)↔C(13)/C(14) (*i.e.* A↔D), while the four carbonyls C(16), C(17), C(19), C(110) (signals B) would not change their chemical environment, and hence remain relatively sharp. Further insight into the carbonyl exchange mechanisms is provided by solid-state ^{13}C EXSY (exchange spectroscopy) at 306 K shown in Fig. 7, with mixing times of 20 and 200 ms. Unfortunately, due to an accidental overlap of the signal E with a spinning side-band from signal A, there is a strong artefact cross-peak between these two signals (which may of course be obscuring a real chemical exchange cross-peak). It can be seen that there is no significant cross-peak between signals A and D, even with a mixing time of 200 ms, and that signal B is in fact involved in exchange with all other signals. Therefore we can conclude that the rotation of the Fe_2Os triangle does not occur by direct 180° jumps within a relatively rigid carbonyl manifold.

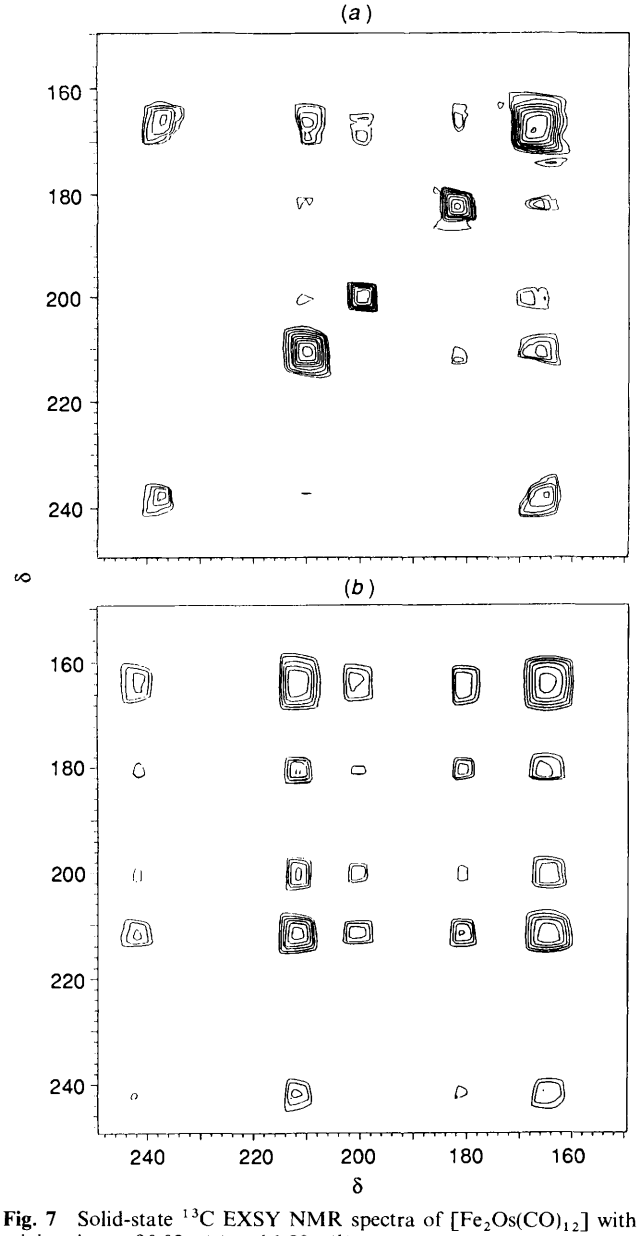

Fig. 7 Solid-state ^{13}C EXSY NMR spectra of $[Fe_2Os(CO)_{12}]$ with mixing times of 0.02 s (*a*) and 0.20 s (*b*)

* The term 'relatively rigid' is used to indicate that the carbonyl ligands retain their relative geometry (and hence the antipodal relationships) but may move to allow relaxation in the transition state. The ligand polyhedron[23] is thus retained intact.

Signal E (due to the two equatorial COs on the osmium atoms) shows strong cross-peaks with *three* other signals B–D. Unless we allow for the extremely unlikely possibility that the two independent molecules of $[Fe_2Os(CO)_{12}]$ exhibit different fluxional behaviour, it is clear that the exchanges observed in the EXSY experiments cannot be explained by a single dynamic process, since two carbonyls cannot exchange with more than two others. The exchange processes in solid $[Fe_2Os(CO)_{12}]$ must be more complicated than indicated by those models presented in the Introduction for the exchange in solid $[Fe_3(CO)_{12}]$. In addition, our NMR evidence now allows us to discount several of these mechanisms as responsible for the observed exchanges in $[Fe_2Os(CO)_{12}]$. In particular, the Johnson model[7] of C_2 libration of the M_3 triangle does not explain the direct exchange between Os- and Fe-bound carbonyls, and the concerted bridge exchange mechanism of Mann[8] is also inconsistent with our results (see below).

The triangular jump mechanism of Hanson[6a,b] provides the most reasonable explanation of our experimental observations, if one assumes that the triangular jump occurs in 60° increments, with a significant (albeit short) residence time in-between the 180° positions. A 60° rotation of the Fe_2Os triangle within a relatively rigid carbonyl manifold generates either a D_3 type all-terminal structure, or a C_2 $[Fe_3(CO)_{12}]$ type structure containing an asymmetric $Fe(\mu\text{-}CO)_2Os$ bridging unit. Neither of these is identical to the ground-state structure, and there is no direct evidence to support either possibility. However, if we assume that the 60° intermediate has the same structure as that of the ground state (there is no evidence for any other structures being present) then the following exchanges are predicted (see Scheme 1): A→(A,B); B→(A,C,E,D); C→(B,C); D→(B,D); E→(B,E). This Scheme requires that any intermediate collapses to the ground-state geometry with the *minimum* of carbonyl reorganisation. Assuming this mechanism is correct, a crude estimate of 2300 ± 300 s^{-1} for the exchange rate may be obtained from the linewidth of signal A at 323 K, giving an activation barrier $\Delta G^{\ddagger} \approx 42(1)$ kJ mol^{-1} for the triangular jump.

While Scheme 1 explains most of the cross-peaks observed, there are extra cross-peaks which are not explained by this mechanism. Those arising between signal C and signals D and E could be due to a component of a direct 120° jump. Such a jump would require a considerable carbonyl reorganisation if the ground-state structure were to be maintained. In addition, there are cross-peaks between signals D and E, which are visible even with the short mixing time of 20 ms. We therefore suggest that there is a second, independent exchange process in solid $[Fe_2Os(CO)_{12}]$ which has a similar energy to the 60° triangular jump process, namely a localised C_2 rotation or trigonal twist of the $Os(CO)_4$ group, which exchanges axial and equatorial sites. Such a low-energy trigonal-twist mechanism in an $Os(CO)_4$ group has been observed in solution in several osmium clusters including $[Os_3(\mu\text{-}H)(\mu_3\text{-}CPh)(CO)_{10}]$.[24]

Finally we note that recent molecular dynamics calculations by Sironi[25] on $[Fe_3(CO)_{12}]$ indicate that in-plane 60° jumps of the Fe_3 triangle have an activation barrier of ≈50 kJ mol^{-1}. These theoretical calculations are hence in accord with our experimental results on $[Fe_2Os(CO)_{12}]$.

Comments on the solid-state ^{13}C NMR spectra of $[Fe_3(CO)_{12}]$

The demonstrable dynamic nature of the disorder in $[Fe_2Os(CO)_{12}]$ has clear implications for $[Fe_3(CO)_{12}]$, in view of the great similarity in molecular *and* crystal structures for the two related clusters. It would seem highly probable that the disorder observed in the crystal structure[9,10] of $[Fe_3(CO)_{12}]$ is also dynamic in nature, and this is consistent with the variable-temperature ^{13}C MAS NMR study by Hanson *et al.*[6a] They showed that the spectra are significantly temperature dependent, indicating some dynamic behaviour, but the interpretation has been subject to controversy. The crux of this controversy lies in the supposed 'anomalous' chemical shift of the bridging carbonyls. A pair of resonances (at δ 238.8 and 236.5) which Hanson *et al.*[6a] assign to the two bridging carbonyls at −93 °C collapse on warming by exchange with a pair of terminal carbonyl ligands, giving rise to a pair of *averaged* signals at δ 224.5 and 226.1 at ambient temperature. In an independent study, Walter *et al.*[6c] have shown that the exchange-averaged shielding tensors and T_1 values for these *averaged* resonances at δ 224.5 and 226.1 are entirely consistent with the interpretation of Hanson *et al.*[6a] However, on the basis of chemical shifts found for several tertiary phosphine derivatives of $[Fe_3(CO)_{12}]$, Mann and co-workers[8] have disputed that the signals at δ 238.8 and 236.5 arise from the bridging carbonyls, and have suggested an alternative interpretation for the ^{13}C NMR data, with a mechanism involving concerted bridge opening and closing which is still rapid at −93 °C. In view of our observations of a static chemical shift of δ ≈240 for the bridging carbonyls in **2**, it is clear that the interpretations of Hanson,[6a] Walter[6c] *et al.* regarding this point are correct. Sironi[25] has suggested that the 'anomalous' chemical shift of the bridging carbonyl may arise from a very low-energy C_2 libration, which results in a rapid averaging of semibridging and symmetric bridging carbonyl sites.

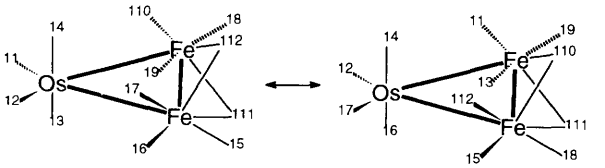

Scheme 1

Conclusion

We have demonstrated that the disorder of the metal atoms in $[Fe_2Os(CO)_{12}]$ first reported by Churchill and Fettinger,[11] is dynamic in nature, and probably occurs by steps of 60°, although only the 180° step has a significant residence time. At 373 K $[Fe_2Os(CO)_{12}]$ adopts a different crystal structure with a unit cell similar to that of $[Fe_3(CO)_{12}]$. Solid-state ^{13}C NMR spectra of $[Fe_2Os(CO)_{12}]$ are consistent with two exchange processes of similar energy, a 60° triangular jump within a relatively rigid carbonyl manifold, and a process involving localised axial–equatorial exchange in the $Os(CO)_4$ group.

Experimental

The cluster $[Fe_2Os(CO)_{12}]$ was prepared by the literature method[18] and was enriched for the ^{13}C NMR studies by stirring in toluene solution at room temperature for 48 h under a ^{13}CO (99% ^{13}C) atmosphere. The solution ^{13}C NMR spectra were obtained in CD_2Cl_2 solution on a Bruker AM200 spectrometer, and the solid-state ^{13}C spectra on a Varian VXR300 spectrometer by the EPSRC Solid State NMR Service, Durham, UK.

X-Ray structural studies

Details of data collection procedures and structure refinement are given in Table 5. Data at 292 and 120 K were collected at Glasgow, those at 223, 288 and 323 K in Bologna. Different crystal specimens were used for the data sets at 120, 223 and 292 K, while the specimen used for the 223 K data set was also used to collect data at 288 and 323 K. No phase change was noted between 100 and 323 K, but there is an apparent phase change around 373 K (see above). As far as possible, all data sets were treated in a similar fashion. Absorption corrections were

Table 5 Experimental details of crystallographic studies

T/K	323	292	288	223	120
a/Å	8.378(4)	8.3573(7)	8.337(6)	8.265(3)	8.2192(9)
b/Å	22.767(8)	22.651(3)	22.609(7)	22.434(7)	22.289(3)
c/Å	8.941(3)	8.932(2)	8.924(5)	8.894(3)	8.843(1)
β/°	96.55(3)	96.55(1)	96.48(5)	96.24(3)	96.23(1)
U/Å^3	1694(1)	1679.9(4)	1671(2)	1639.3(10)	1610.5(3)
θ range for cell/°	9.0–14.0	17.5–20.0	9.0–14.0	9.0–14.0	20.8–32.1
D_c/g cm^{-3}	2.502	2.523	2.536	2.585	2.631
μ(Mo-Kα)/cm^{-1}	92.35	93.12	93.60	95.4	97.14
Scan angle/°	0.90 + 0.35 tan θ	0.95 + 0.46 tan θ	0.90 + 0.35 tan θ	0.80 + 0.35 tan θ	0.8 + 0.8 tan θ
2θ range/°	3.0–25.0	2.26–30.0	3.0–27.0	3.0–25.0	2.49–30.0
Crystal size/mm	0.12 × 0.15 × 0.16	0.3 × 0.25 × 0.10	0.12 × 0.15 × 0.16	0.12 × 0.15 × 0.16	0.35 × 0.35 × 0.3
Method of absorption correction	ψ scan	ψ scan	ψ scan	ψ scan	DIFABS
Range of transmission coefficients	1.000–0.787	0.984–0.477	1.000–0.332	1.000–0.366	0.895–1.229
No. of data collected	2984	5321	3969	3170	5098
No. of unique data	2908	5202	3874	3085	4978
hkl ranges	−9 to 9, 0–27, 0–8	−11 to 0, −31 to 0, −12 to 12	−10 to 10, 0–28, 0–11	−9 to 9, 0–26, 0–10	−12 to 12, −34 to 0, 0–13
R_{sigma} {$= \Sigma[\sigma(F_o^2)]/\Sigma(F_o^2)$}	0.034	0.030	0.022	0.017	0.012
Standard reflections	(4, 8, 2), (−2, 4, −2), (0, −4, −4)	(−1, −14, −1), (5, −1, 0), (0, −1, 5)	(−3, −3, −1), (−2, 4, −2), (1, −3, −4)	(−3, −3, −1), (−2, 4, −2), (1, −3, −4)	(0, 5, 4), (−1, 10, −2), (8, −2, 1)
No. of data in refinement	2908	5199	3848	3077	4965
No. of refined parameters	337	513	511	489	486
Final R [$I > 2\sigma(I)$]	0.078	0.039	0.037	0.032	0.032
(all data)	0.110	0.062	0.051	0.035	0.039
R'^2 [$I > 2\sigma(I)$]	0.241	0.102	0.097	0.086	0.078
(all data)	0.268	0.116	0.122	0.092	0.105
Flack absolute structure parameter	0.07(4)	0.10(1)	0.11(2)	0.14(1)	0.17(1)
Goodness of fit S	1.16	1.08	1.00	1.09	1.24
Largest remaining feature in electron-density map (maximum, minimum)/e Å^{-3}	1.55, −2.15	1.41, −2.29	1.65, −1.69	1.90, −1.10	2.51, −2.58
Shift/e.s.d. in last cycle (mean, maximum)	0.059, 0.555	0.0001, 0.001	0.079, −0.569	0.042, 0.523	0.0005, 0.002

Details in common: M = 638.02; monoclinic; space group Pn; Z = 4; $F(000)$ = 1184; scan mode ω–2θ.

carried out using semiempirical ψ scans, except for the data set at 120 K for which the ψ-scan data set proved inadequate. For this data set alone the method of Stuart and Walker[26] was used. A careful comparison of both methods of absorption correction for the data set collected at 292 K revealed no significant differences in the final refined positional and thermal parameters. Refinement against F_o^2 was carried out using the program SHELXL 93.[27]

Structure determinations. *At 292 K.* A single crystal of suitable size was attached to a glass fibre using acrylic resin, and mounted on a goniometer head in a general position. Data were collected on an Enraf-Nonius Turbo CAD4 diffractometer, running under CAD4-Express software, and using graphite-monochromated X-radiation (λ = 0.710 73 Å).

Accurate unit-cell dimensions were determined by refinement of the setting angles of 25 optimum high-angle reflections, which were flagged during data collection. Standard reflections were measured every 2 h during data collection; a decay of *ca.* 1.8% was noted and an interpolated correction was applied to the reflection data. Lorentz-polarisation corrections, and an absorption correction (semiempirical ψ scans based on nine reflections with χ angles greater than 85°), were then applied to the reflection data. The starting atomic coordinates were taken from the previously reported determination by Churchill and Fettinger.[11] All atoms, apart from the metals in the minor component Fe_2Os triangle, were allowed anisotropic thermal motion. No attempt was made to obtain the C and O positions for the minor component. The site occupancies of the major and minor components of the metal triangles in the two crystallographically independent molecules were refined as independent variables, giving occupancies for the major orientation of 91 and 93% repectively for molecules 1 and 2. An investigation into possible Fe/Os disorder at each metal site showed that none was detectable for the major components in both of the independent molecules. This was also the case for the minor component of molecule 2, while for the minor component of molecule 1 the relative proportions of the three possible orientations were found to be 7.5(3):1.9(2):1.9(3). Allowing for this further disorder modifies the overall major:minor populations, such that for molecule 1 the major orientation comprises 88.5(3)% of the total, while for 2 the major orientation comprises 93.5(3)%. An extinction correction was also applied. Refinement was by full-matrix least squares on F_o^2, using the weighting scheme $w = [\sigma^2(F_o^2) + (0.0719P)^2 + 0.833P]^{-1}$ where $P = [F_o^2/3 + 2F_c^2/3]$; $\sigma(F_o^2)$ was estimated from counting statistics. Neutral atom scattering factors, values of f' and f'' and atomic absorption coefficients were taken from Tables 6.1.1.4, 4.2.6.8 and 4.2.4.2 respectively of ref. 28.

At 120 K. All the above details were the same except the following. The crystal was mounted using silicone grease in a 0.5 mm Lindemann tube. The sample was cooled using an Oxford Cryosystems Cryostream unit, with the crystal temperature held at 120 ± 2 K for the duration of data collection. A decay of ≈8% in the standard intensities was observed, and the data set corrected for decomposition by a linear interpolation. No disorder in the metal positions was discernible. All atoms were allowed anisotropic thermal motion. The weighting scheme used was $w = [\sigma^2(F_o^2) + (0.0291P)^2 + 20.162P]^{-1}$.

At 223 K. All the details as for the 292 K data collection were the same except the following. The sample was cooled using an Enraf-Nonius variable-temperature device, with the crystal temperature held at 223 ± 2 K for the duration of data collection. No significant variation in the standard intensities was observed. No disorder in the metal positions was discernible. All atoms were allowed anisotropic thermal

motion. The weighting scheme used was $w = [\sigma^2(F_o^2) + (0.0784P)^2 + 5.283P]^{-1}$.

At 288 K. All the details as for the 292 K data collection were the same except the following. No significant variation in the standard intensities was observed. The weighting scheme used was $w = [\sigma^2(F_o^2) + (0.0767P)^2 + 6.029P]^{-1}$.

At 323 K. All the details as for the 292 K data collection and refinement were the same except the following. The sample was heated using an Enraf-Nonius variable-temperature device, with the crystal temperature held at 323 ± 2 K for the duration of data collection. No significant variation in the standard intensities was observed. An initial careful refinement to analyse for possible metal site disorder indicated that for the sites labelled as iron atoms in Fig. 4 there was no more than 3% of an osmium atom present. Henceforth a single elemental species was assigned to each of the metal sites as indicated in Fig. 4. The metal atoms were refined with anisotropic thermal parameters, with all C and O atoms refined with isotropic thermal parameters. The light-atom positions were poorly determined, and the C–O distances were constrained to be 1.15 Å. Several of the light atoms were disordered over two sites. The weighting scheme used was $w = [\sigma^2(F_o^2) + (0.1801P)^2 + 8.56P]^{-1}$.

Complete atomic coordinates, thermal parameters and bond lengths and angles have been deposited at the Cambridge Crystallographic Data Centre. See Instructions for Authors, *J. Chem. Soc., Dalton Trans.*, 1996, Issue 1. Tables of observed and calculated structure factors are available from L. J. F. on request.

EXAFS measurements

All EXAFS data were collected at the Daresbury synchrotron radiation source (SRS) on stations 7.1 and 9.2 in transmission mode at the Os L_{III} edge, and in fluorescence mode at the Fe K edge (using a manganese foil to absorb scattered radiation). The solid samples were diluted with boron nitride in order to achieve changes in log (I_0/I) in the range 1–1.5 at the absorption edge. Tetrahydrofuran solution samples were collected in cells of pathlength *ca.* 3 mm. The raw data were treated as previously described.[29] Three to four repeat spectra were summed for each sample to improve signal-to-noise ratios. The temperature of measurement was controlled by an Oxford Instruments cryostat system (stable to *ca.* 0.1°). All iron edge models were essentially identical. The Fe–Os shell was fitted easily, but the Fe–Fe contact was less well fitted, with quite large errors in R and the Debye–Waller factor A. There was a relatively wide variation between the different spectra, probably because the Fe–Os contact was compensating for the Fe–Fe contacts, and the refined Fe–Fe distances were marginally lower than those that were observed in the X-ray diffraction experiments. Multiple scattering was used for the Fe–C–O unit. Two possibilities for modelling the iron data were examined; either two Fe–C (and two Fe–O) shells, one for the three terminal COs and one for the two bridging COs, or a single shell for all carbonyls. The first option gave the best fit. For this case refinement of the Fe–C–O angle gave a value around 195(2)°, with an accompanying decrease in fit index of 10–20%. Addition of a separate Fe–C shell at between 2 and 2.1 Å did not improve the model. In conclusion, the bridging Fe–CO contact cannot be properly fitted, presumably because there is too much variation in the four Fe–C distances, resulting in an averaging of the signal. The refined Fe–C and Fe–O distances for the terminal Fe–CO unit are very similar to the X-ray diffraction data, suggesting that the bridging COs are not contributing to this shell. All the models used for the Os L_{III} edge data were essentially the same, with four Os–C, four Os–O, and two Os–Fe shells. The refined Os–Fe distances for the solid samples were slightly shorter than in the single-crystal diffraction data, but not significantly so. In the solution and frozen-solution data an extra peak in the Fourier transform was observed at *ca.* 4.3 Å. This was modelled by four Os · · · C contacts arising from the $Fe(CO)_4$ units. Despite the high correlations between some refined parameters (see Table 3), the derived distances are generally in good agreement with the X-ray diffraction results.

Acknowledgements

We thank the EPSRC (UK) and Ministero dell'Universitá e della Ricerca Scientifica e Tecnologica (Italy) for financial support. Dr. D. Apperley (EPSRC Solid State NMR Service, Durham, UK) is thanked for his help in obtaining the solid-state ^{13}C NMR spectra.

References

1 E. Band and E. L. Muetterties, *Chem. Rev.*, 1978, **78**, 639; B. F. G. Johnson and R. E. Benfield, in *Transition Metal Clusters*, ed. B. F. G. Johnson, Wiley, Chichester, 1980, ch. 7.
2 S. Aime, R. Gobetto, A. Orlandi, C. J. Groombridge, G. E. Hawkes, M. D. Mantle and K. D. Sales, *Organometallics*, 1994, **13**, 2375; B. E. Hanson, M. J. Sullivan and R. J. Davis, *J. Am. Chem. Soc.*, 1984, **106**, 251; B. E. Hanson and E. C. Lisic, *Inorg. Chem.*, 1986, **25**, 716; S. Aime, M. Botta, R. Gobetto and B. E. Hanson, *Inorg. Chem.*, 1989, **28**, 1196.
3 *The Synergy between Dynamics and Reactivity at Clusters and Surfaces*, NATO ASI Ser. C, ed. L. J. Farrugia, Kluwer, Dordrecht, 1995, vol. 465.
4 D. Braga, *Chem. Rev.*, 1992, **92**, 633 and refs. therein.
5 F. A. Cotton and D. L. Hunter, *Inorg. Chim. Acta*, 1974, **11**, L9; F. A. Cotton and B. E. Hanson, *Isr. J. Chem.*, 1977, **15**, 165.
6 (*a*) B. E. Hanson, E. C. Lisic, J. T. Petty and G. A. Iannaconne, *Inorg. Chem.*, 1986, **25**, 4062; (*b*) H. Dorn, B. E. Hanson and E. Motel, *Inorg. Chim. Acta*, 1981, **54**, L71; (*c*) T. H. Walter, L. Reven and E. Oldfield, *J. Phys. Chem.*, 1989, **93**, 1320.
7 (*a*) B. F. G. Johnson, *J. Chem. Soc., Chem. Commun.*, 1976, 703; (*b*) B. F. G. Johnson and A. Bott, *J. Chem. Soc., Dalton Trans.*, 1990, 2437; (*c*) D. Braga, C. E. Anson, A. Bott, B. F. G. Johnson and E. Marseglia, *J. Chem. Soc., Dalton Trans.*, 1990, 3517; (*d*) B. F. G. Johnson, Y. V. Roberts and E. Parsini, *J. Chem. Soc., Dalton Trans.*, 1992, 2573.
8 H. Adams, N. A. Bailey, G. W. Bentley and B. E. Mann, *J. Chem. Soc., Dalton Trans.*, 1989, 1831.
9 D. Braga, F. Grepioni, L. J. Farrugia and B. F. G. Johnson, *J. Chem. Soc., Dalton Trans.*, 1994, 2911.
10 F. A. Cotton and J. M. Troup, *J. Am. Chem. Soc.*, 1974, **96**, 4155.
11 M. R. Churchill and J. C. Fettinger, *Organometallics*, 1990, **9**, 446.
12 D. Braga, L. J. Farrugia, F. Grepioni and A. M. Senior, *J. Chem. Soc., Chem. Commun.*, 1995, 1219.
13 L. J. Farrugia, *Acta Crystallogr., Sect. C*, 1991, **47**, 1310.
14 M. I. Bruce, M. J. Liddell, O. Bin Shawkataly, C. A. Hughes, B. W. Skelton and A. H. White, *J. Organomet. Chem.*, 1988, **347**, 207.
15 A. J. Deeming, S. Donovan-Mtunzi, K. I. Hardcastle, S. E. Kabir, K. Hendrick and M. McPartlin, *J. Chem. Soc., Dalton Trans.*, 1988, 579.
16 (*a*) V. G. Albano and D. Braga, in *Accurate Molecular Structures: Their Determination and Importance*, eds. A. Domenicano and I. Hargittai, Oxford University Press, 1992, pp. 530–553; (*b*) D. Braga, F. Grepioni, P. J. Dyson, B. F. G. Johnson, P. Frediani, M. Bianchi and F. Piacenti, *J. Chem. Soc., Dalton Trans.*, 1992, 2565; (*c*) V. G. Albano, D. Braga and F. Grepioni, *Acta Crystallogr., Sect. B*, 1989, **45**, 60.
17 D. Braga, F. Grepioni, C. M. Martin, E. Parsini, P. J. Dyson and B. F. G. Johnson, *Organometallics*, 1994, **13**, 2170.
18 W. A. G. Graham and J. R. Moss, *J. Organomet. Chem.*, 1984, **270**, 237.
19 N. Binstead, S. J. Gurman and J. W. Campbell, EXCURV92, Daresbury Laboratory, 1992.
20 M. M. Maricq and J. S. Waugh, *J. Chem. Phys.*, 1979, **70**, 3300.
21 (*a*) S. Aime, M. Botta, R. Gobetto and A. Orlandi, *Magn. Reson. Chem.*, 1990, **28**, S52; (*b*) G. E. Hawkes, K. D. Sales, S. Aime, R. Gobetto and L.-Y. Lian, *Inorg. Chem.*, 1991, **30**, 1489.
22 S. Aime, M. Botta, R. Gobetto, D. Osella and L. Milone, *Inorg. Chim. Acta*, 1988, **146**, 151.
23 B. F. G. Johnson and Y. V. Roberts, *Polyhedron*, 1993, **12**, 977.
24 W.-Y. Yeh, J. R. Shapley, Y.-J. Li and M. R. Churchill, *Organometallics*, 1985, **4**, 767.

25 A. Sironi, unpublished work.
26 N. Walker and D. Stuart, *Acta Crystallogr., Sect. A*, 1983, **39**, 158.
27 G. M. Sheldrick, SHELXL 93, Program for Crystal Structure Refinement, University of Göttingen, 1993.
28 *International Tables for X-Ray Crystallography*, Kluwer, Dordrecht, 1995, vol. C.
29 D. Ellis, L. J. Farrugia, P. Wiegeleben, J. G. Crossley and A. G. Orpen, *Organometallics*, 1995, **14**, 481.

Received 17*th August* 1995; *Paper* 5/06038I